Microstructure Evolution of On-substrate NiTi Shape Memory Alloy Thin Films

Xi Wang[1], Ann Lai[1], Joost J. Vlassak[1], and Yves Bellouard[2]
[1]Division of Engineering and Applied Sciences, Harvard University, Cambridge, MA 01238 USA
[2]Center for Automation Technologies, Rensselaer Polytechnic Institute, Troy, NY 12180 USA

ABSTRACT

When deposited at room temperature, sputtered NiTi thin films are amorphous and need to be crystallized before they can be used as a functional material. We present the results of an annealing study on substrate-constrained NiTi shape memory thin films. Amorphous films of a NiTi shape memory alloy were deposited by UHV sputtering. Films of thickness 1.0 μm were grown on (100) Si wafers both with and without an LPCVD SiNx barrier. The as-deposited films were annealed in vacuum at temperatures ranging from 500°C to 800°C. The microstructure of the annealed films was characterized using transmission electron microscopy (TEM), energy dispersive X-ray spectroscopy (EDX), and Rutherford back scattering (RBS).

INTRODUCTION

Among shape memory alloys, NiTi alloys have received the most attention. NiTi-based thin films are excellent candidates for use as actuator materials in microelectronmechanical system (MEMS) applications [1-4]. The microstructure evolution of free-standing NiTi films after heat treatment has been studied in detail by Ishida *et al*. [5-7]. However, the film thickness that they investigated is approximately 8 μm, and some applications may require submicron films. Furthermore, the interaction of very thin films with the substrate is unknown and needs to be studied. In the present study, the microstructure of 1 μm on-substrate NiTi thin films is investigated in relation to their heat treatment.

EXPERIMENTAL DETAILS

Thin films of NiTi were deposited by means of UHV d.c. magnetron sputtering at 200W with a base pressure of less than 5.0×10^{-8} Torr and Ar pressure of 3.0 mTorr. The deposition rate was about 0.5 μm/h. The substrates used were (100) Si wafers with and without an LPCVD SiN_x barrier layer. The thickness of SiN_x layer was approximately 2000Å. The NiTi thickness was approximately 1 μm. The film composition was Ni-49.5at%Ti as determined by Electron Microprobe analysis (EMPA). After the deposition, the films were annealed in a quartz vacuum furnace at four different temperatures, 500, 600°C, 700°C and 800°C for 1 hour and then furnace-cooled to room temperature before removal. The pressure during the heat treatment was below 5×10^{-6} Torr while the heating and cooling rates were approximately 40 °C/min and 10°C/min, respectively.

The film composition after heat treatment was determined by EMPA. The energy of the electron beam was chosen at 10 KeV to ensure activation of the characteristic X-ray without penetrating the substrate significantly. The composition-depth profile of the films before and after heat treatment were ascertained by Rutherford back scattering (RBS) using a He^{2+} beam with an energy of 2.0 MeV. The crystal structure of the annealed film was identified by X-ray diffractometry. The microstructure of the films was observed with transmission electron microscopy (TEM) and energy dispersive X-ray spectroscopy (EDX).

RESULTS AND DISCUSSION

After the heat treatment, the surface morphology of the films was examined using optical microscopy. All films were free of cracks except the films on Si substrate annealed at 700°C and 800°C which exhibited "mud" type cracking as shown in Figure 1. In addition, there are many dark spots in the 800°C films on Si substrate. The film compositions determined by EMPA are listed in Table 1 and 2. For the films on Si substrates, the films with cracks are not listed. The Si content of the films increases with increasing annealing temperature as the film reacts with the Si substrate to form silicides. Stemmer *et al.* [8] reported that this reaction occurs even at relative low annealing temperature of about 525°C. During annealing, Ni diffuses into the Si substrate to form nickel silicide, and Si diffuses into the alloy to form a ternary silicide [8,9]. The formation of silicides as observed in the films on Si substrate annealed at higher temperatures may have either embrittled the film or increased the tensile stress facilitating the cracking.

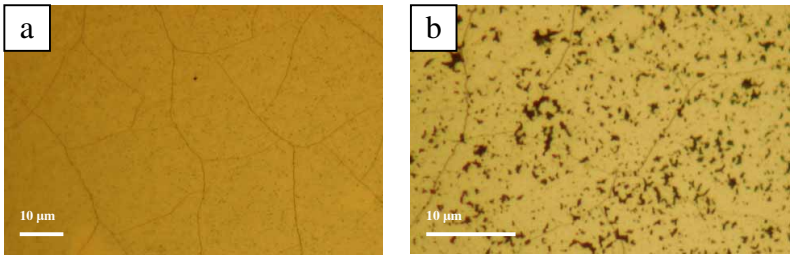

Figure 1. Optical micrographs of NiTi films on Si substrate show cracking: (a) 700°C, (b) 800°C.

RBS spectra are shown in Figure 2. The computer simulation (XRUMP) of the energy spectrum shows that as-deposited films are $Ti_{49.5}Ni_{50.5}$ for either substrate, which is consistent with the EMPA results. The profiles of annealed films are too complicated to be simulated exactly. However, a comparison of the annealed films with as-deposited films on Si substrate shows that significant reaction occurs at the interface at a relative low temperature between 500°C and 600°C. For films on the Si/SiN_x substrates, reaction with the substrate occurs for the films annealed at 700°C and 800°C, although the extent is much more limited. Finally, the peak in the spectrum associated with the surface of the films is due to the oxidation during the annealing.

Table 1. The film compositions on Si substrate

Temperature	Si at.%	Ti at.%	Ni at.%
As-deposited	0.08	49.47	50.45
500°C	0.14	49.24	50.62
600°C	0.88	57.09	42.03

Table 2. The film compositions on Si/SiN_x substrate

Temperature	Si at.%	Ti at.%	Ni at.%
As-deposited	0.07	49.43	50.50
500°C	0.18	49.52	50.30
600°C	0.38	47.99	51.63
700°C	2.18	52.73	45.09
800°C	8.97	51.99	39.04

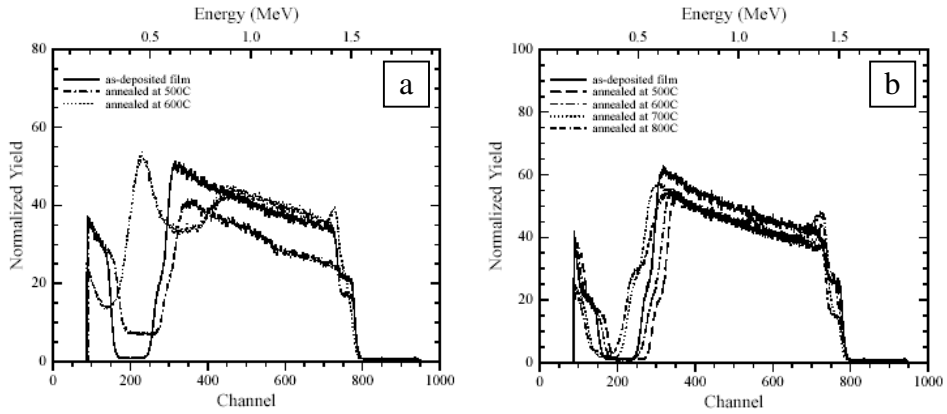

Figure 2. RBS spectra of TiNi films: (a) on Si, (b) on Si/SiNx.

The room-temperature X-ray diffraction patterns of the annealed films are shown in Figure 3. There is a R-phase peak at the high angle side of the (110) peak of B_2 phase for the film annealed at 500°C, which is verified by TEM results. Also, there is a small amount of Ni_4Ti_3. With increasing annealing temperature, this R-phase peak decreases, and a peak corresponding to Ni_3Ti at $2\theta=46.6^o$ appears. According to a study of bulk NiTi alloys by Nishida *et al.* [10], Ni_4Ti_3 is a metastable phase and phase separations occur with aging to form the stable Ni_3Ti phase. These authors, however, found no Ni_3Ti in bulk samples held below 750°C for a short period of time. Since the crystallization activation energy of sputtered NiTi thin film is smaller than that of the bulk materials [11], the precipitation process may also be easier in thin films. This indicates that more careful consideration of annealing temperature and time is needed when crystallizing the NiTi thin films. The suppression of R-phase transformation in the films annealing at high temperature may be due to the formation of Ni_3Ti precipitates and the increased surface oxidation and interfacial reaction.

The microstructure of films on Si/SiN_x substrate was investigated by TEM and energy dispersive X-ray spectroscopy (EDX) as a function of annealing temperature. Generally, the annealed films have a layered structure with oxide layers on the surface of the film (top-layer), several layers of reaction products at the interface of NiTi film and substrate (bottom-layer), and a layer of NiTi compound phases in between (mid-layer).

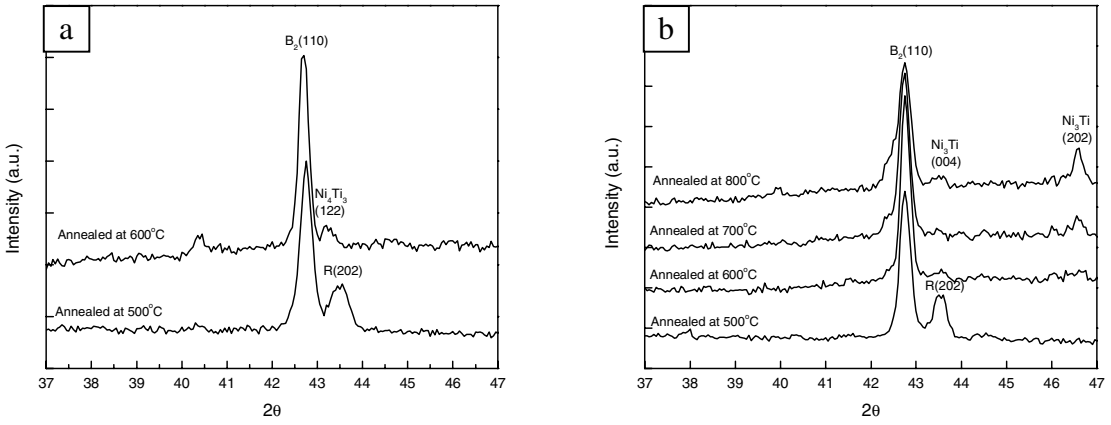

Figure 3. R.T. X-ray diffraction pattern of annealed films: (a) on Si, (b) on Si/SiN_x.

Figure 4(a) shows the cross-section TEM micrograph of the NiTi film on Si/SiN_x substrate annealed at 800°C. The film has a columnar grain structure, with a grain size of about 0.4 μm. At least two layers each can be distinguished at the film-substrate interface and at the film surface. During sample preparation, some interface layers were broken and some were ion-milled away. Figure 4(b) and (c) shows the TEM micrographs of the two top oxide layers, which are TiO and Ti_4Ni_2O, respectively, as determined from d-spacings obtained from selected area diffraction. The gain size of those layers increase with increasing annealing temperature.

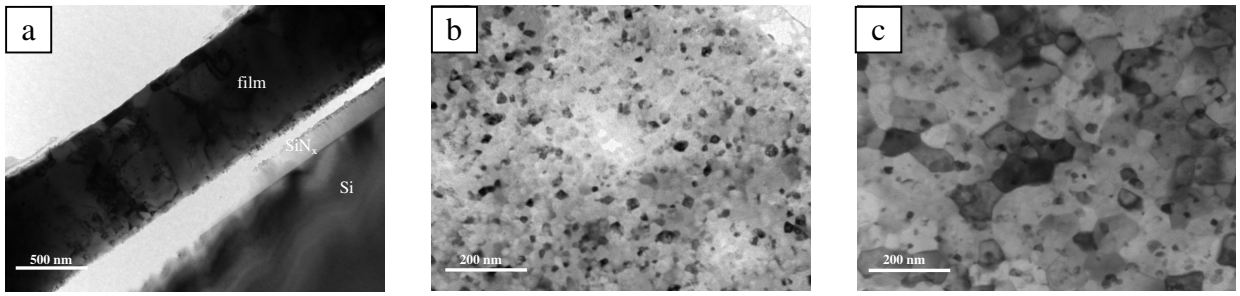

Figure 4. (a) Cross-section TEM micrograph of NiTi film on Si/SiN_x annealed at 800°C. Oxide layers and interfacial reaction products layers are clearly seen. (b),(c) Microstructure of the surface oxide layer in 800°C film: (b) topmost layer, TiO, (c) 2nd top layer, Ti_4Ni_2O.

Figures 5(a) and (b) show bright-field images and the corresponding diffraction patterns of 500°C film. The 600°C films have the similar results. The diffraction pattern is consistent with a mixture of the $[111]_{B2}$, $[0001]_R$ and $[111]_{Ni4Ti3}$ zones. For 700°C and 800°C films, there are only two phases in the mid-layer: B_2 and Ni_3Ti. Figures 5 (c) and (d) show the bright-field image of a

big Ni_3Ti grain through the film thickness in 800°C film and the corresponding diffraction pattern. Figures 5 (e) and (f) show a B_2 grain and the corresponding electron diffraction pattern in the 800°C film — no R-phase is present. Figure 6 shows a STEM image and EDX spectra for a cross-section of the 800°C film. Grains I and II in the STEM image correspond to Ni_3Ti and B_2 grains respectively according to EDX results. Figure 6 (a) indicates that Ni_3Ti nucleates at the top surface and grows toward the film/substrate interface while consuming the B_2 matrix. This happens as a result of surface oxidation since the ensuing change in local Ti/Ni ratio facilitates Ni_3Ti nucleation. Formation of phases other than the B_2 phase at the interface with the substrate and at the surface of the films reduces the amount of material that can undergo the martensitic transformation and thus decrease the effectiveness of the film as an actuator material.

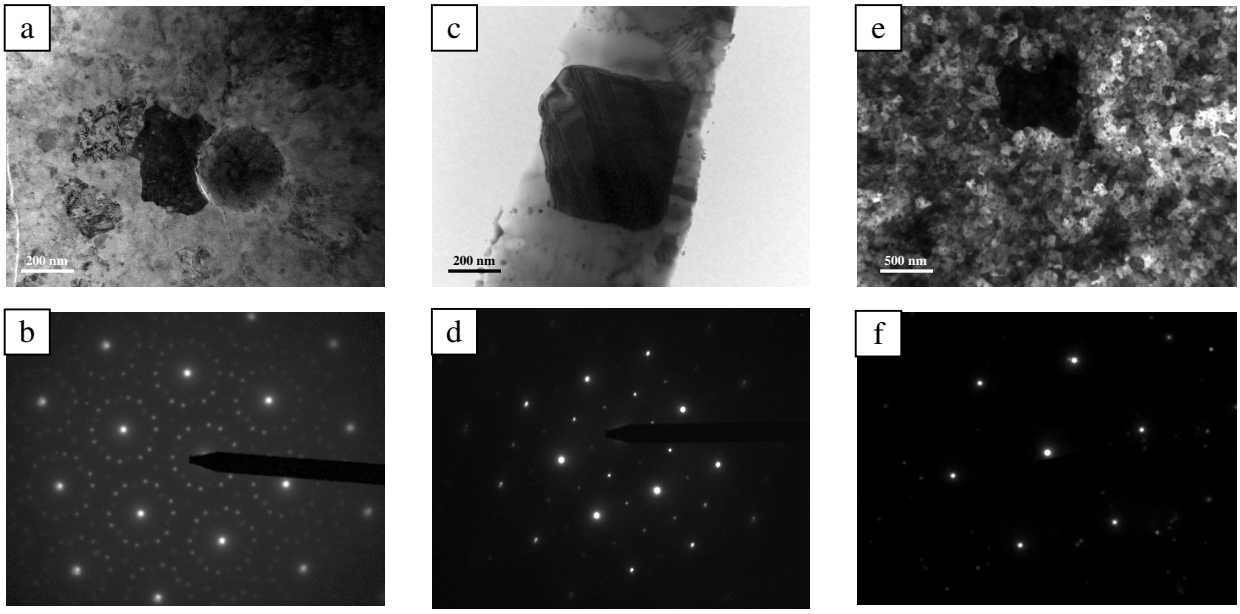

Figure 5. (a) Bright-field image and (b) electron diffraction pattern of grain in the 500°C film. The electron beam is parallel to $[111]_{B2}$ zone axis. (c) Bright-field image and (d) electron diffraction pattern of large Ni_3Ti grain in the 800°C film. The electron beam is parallel to $[-111]_{Ni3Ti}$ zone axis. (d) Bright-field image and (e) electron diffraction pattern of B_2 grain in the 800°C film. The electron beam is parallel to $[111]_{B2}$ zone axis.

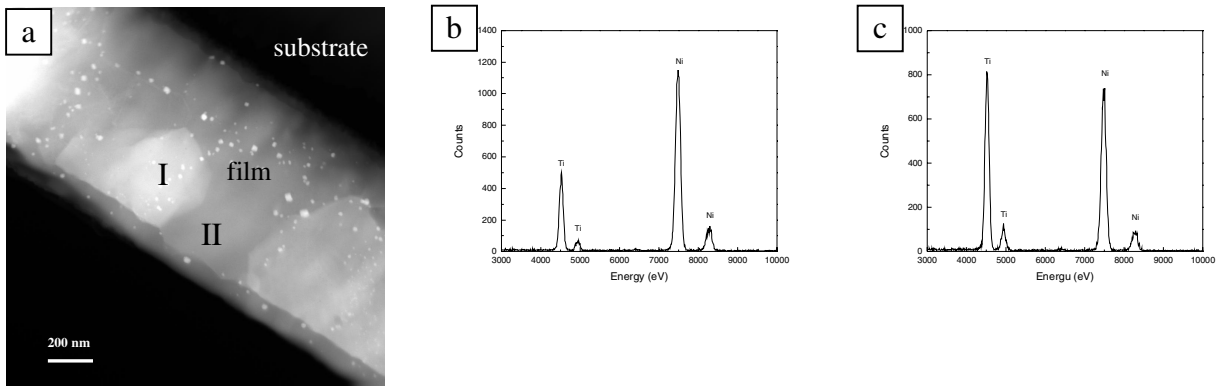

Figure 6. (a) Scanning transmission electron micrograph of cross-sectional 800°C film, (b) and (c) EDX spectra taken from region labeled I and II in (a).

CONCLUSIONS

Amorphous thin films of Ni-49.5at%Ti alloys were deposited onto (100) Si wafer with and without a thin LPCVD SiN_x barrier layer. The films were annealed in vacuum at various temperatures. The films were annealed in vacuum at various temperatures. Significant interfacial reaction occurs between the NiTi and Si for films without barrier, while SiN_x acts as a good barrier layer up to 700°C. Films annealed at lower temperatures do not form silicides and the resulting microstructure is much more homogenous. In addition, surface oxidation can cause the nucleation of Ni_3Ti near the oxide layer. Large Ni_3Ti grains in films annealed at high temperature along with the surface oxide and interfacial reaction products severely limit the martensitic transformation of the austenite.

ACKNOWLEDGMENTS

Financial support from the Division of Engineering and Applied Sciences at Harvard University, from the Harvard MRSEC (DMR-98-09363), and from the National Science Foundation (DMR-0133559; DMR-0215902) is gratefully acknowledged. The electron microscopy analysis was completed using the facilities of the Center for Imaging and Mesoscale Structure (CIMS) at Harvard University. Y. Bellouard is supported by the New York State Office for Science, Technology and Academic Research (NYSTAR).

REFERENCES

1. A.P. Lee, D.R. Ciarlo, P.A. Krulevitvh, S. Lehew, J. Trevino and M.A. Northup, *Sensors and Actuators A* **54**, 755 (1996).
2. M. Kohl, D. Dittmann, E. Quandt and B. Winzek, *Sensors and Actuators A* **83**, 214 (2000).
3. E. Makino, T. Mitsuya and T. Shibata, *Sensors and Actuators A* **88**, 256 (2001).
4. J.J. Gill, D.T. Chang, L.A. Momoda and G.P. Carman, *Sensors and Actuators A* **93**, 148 (2001).
5. A. Ishida, M. Sato, A. Takei and S. Miyazaki, *Mater. Trans. JIM.* **36**, 1349 (1995).
6. A. Ishida, M. Sato, A. Takei, K. Nomura and S. Miyazaki, *Metall. Mater. Trans. A* **27A**, 3753 (1996).
7. A. Ishida, K. Ogawa, M. Sato and S. Miyazaki, *Metall. Mater. Trans. A* **28A**, 1985 (1997).
8. S. Stemmer, G. Duscher, C. Scheu, A.H. Heuer and M. Ruhle, *J. Mater. Res.* **12**, 1734 (1997).
9. L.S. Hung and J.W. Mayer, *J. Appl. Phys.* **60(3)**, 1002 (1986)
10. M. Nishida, C.M. Wayman, and T. Honma, *Metall. Trans. A* **17A**, 1505 (1986).
11. J.Z. Chen and S.K. Wu, *Thin Solid Films* **339**, 194 (1999).